Eur. Phys. J. B **46**, 441–447 (2005)
DOI: 10.1140/epjb/e2005-00268-2

THE EUROPEAN PHYSICAL JOURNAL B

Evaluation of hydrogen chemisorption in nanostructured carbon films by near edge X-ray absorption spectroscopy

C. Lenardi[1,4,a], M. Marino[2], E. Barborini[3,4], P. Piseri[3,4], and P. Milani[3,4]

[1] Istituto di Fisiologia Generale e Chimica Biologica, Università di Milano, via Trentacoste 2, 20134 Milano, Italy
[2] Dipartimento di Matematica, Università di Milano, via Saldini 50, 20133 Milano, Italy
[3] Dipartimento di Fisica, Università di Milano, Via Celoria 16, 20133 Milano, Italy
[4] Centro Interdisciplinare Materiali e Interfacce Nanostrutturati (CIMAINA), Università di Milano, Via Celoria 16, 20133 Milano, Italy

Received 8 February 2005 / Received in final form 18 May 2005
Published online 18 August 2005 –

Abstract. We have developed a method for the quantitative evaluation of the chemisorbed fraction of hydrogen in nanostructured carbon films using Near Edge X-ray Absorption Spectroscopy (NEXAFS). In the carbon *K*-edge spectrum the peak related to carbon bonded to hydrogen is assumed to be correlated with the amount of hydrogen bonded to carbon. This assumption is supported by a comparative analysis of gas-phase hydrocarbons obtained via Electron Energy Loss Spectroscopy (EELS). We applied the method to nanostructured carbon (ns-C) films synthesized by supersonic cluster beam deposition. The evaluated quantity of chemisorbed hydrogen in different samples exposed to molecular hydrogen (pressure of 0.12 MPa, for 3 hours at room temperature) is ~ 1.5 wt.%.

PACS. 81.05.Uw Carbon, diamond, graphite – 61.46+w Nanoscale materials: clusters, nanoparticles, nanotubes, and nanocrystals – 61.10.Ht X-ray absorption spectroscopy: EXAFS, NEXAFS, XANES, etc.

1 Introduction

In recent years there has been a considerable experimental and theoretical effort in the investigation of nanostructured carbon materials as suitable hydrogen storage medium. The initial experiments have been very promising since a noticeably high hydrogen uptake in nanotubes and nanofibers [1–4] has been claimed, but subsequent attempts to reproduce those data were unsuccessful [5,6]. More recent results have established lower values both for nanotubes [7–14] and for nanofibers [11,14–17], showing that the method of preparation of carbon nanostructures and the uptaking procedure, namely hydrogen pressure and sample temperature, critically affect the final hydrogen sorption. Moreover Hirscher et al. [18] have shown that those large discrepancies can be also explained by the intrinsic difficulty in performing quantitative analysis of the storage capacity on materials available in very low quantities.

The quantitative evaluation of hydrogen uptake is one of the major difficulties in the study of hydrogen storage in carbon materials. The main techniques nowadays applied are: i) volumetric method; ii) thermogravimetric analysis (TGA) and iii) thermal desorption spectroscopy (TDS). The first method is based on the pressure variation both during adsorption and desorption of hydrogen, but it requires a large amount of carbon material (a few hundreds of milligrams) and is very sensitive to any leakage and thermal instability of the experimental apparatus [4,19]. The second technique controls the weight changes of the carbon sample due to adsorption and desorption of hydrogen, but no discrimination of sorption of other gasses can be carried out. Moreover also in this case the required amount of carbon mass is rather high (at least 10 mg) [15]. In the third method hydrogen desorption is evaluated by mass spectrometry in an ultra high vacuum apparatus. This technique is mass selective and highly sensitive, and a moderate quantity of carbon material (≤ 1 mg) can be sufficient for obtaining very accurate results [1,20].
The main drawback of the described methods is the difficulty of determining the amount of hydrogen sorption in very low quantity of carbon as in the case of thin films. Our method, described in detail in the paper, is instead able to overcome this limit, allowing to evaluate hydrogen content also in samples with a mass $< 1\,\mu g$.
Among nanostructured carbon-based materials candidates for hydrogen uptake, nanostructured carbon (ns-C) produced by supersonic cluster beam deposition has been recently studied. Ns-C is characterized by high specific surface area and porosity that can be controlled by varying the cluster production and deposition conditions [21,22]. Ns-C has a density ranging between 1.0 and 1.4 g/cm^3 with a typical specific surface area of about 700 m^2/g and a pore size distribution prevalently in the region with diameter less than 20 Å [23]. The morphology of the films at

[a] e-mail: cristina.lenardi@mi.infn.it,

different length scales has been extensively characterised (see e.g. Ref. [21]): TEM analysis shows the presence of small closed shell particles, graphene sheets, onion- and tubular-like particles, all embedded in an amorphous matrix, while AFM measurements indicate how roughness, scale invariance, and spatial correlation of the film surface depend on cluster precursor size and film thickness.

In a previous work of ours we already studied the hydrogen sorption in ns-C both with TDS and X-ray adsorption [23]. In that case we exposed to molecular hydrogen only films grown with large clusters as precursors. The exposure conditions (0.08 MPa for 30 min) were gentler than those used in this paper, and the largest amount of absorbed hydrogen was evaluated to be approximately 0.5 wt.%. Recently we compared our experimental results with large-scale molecular dynamics simulations, obtaining a good quantitative agreement between the two approaches and the confirmation that hydrogen is mainly chemisorbed on the carbon [24].

In this paper we present and discuss a quantitative method for the evaluation of hydrogen chemisorption in nanostructured carbon materials. The method is founded on the analysis of near edge X-ray absorption (NEXAFS) spectra of ns-C. It is based on the assumption that the $\sigma^*_{\mathrm{C-H}}$ peak is directly related to the amount of H chemically bonded to C thanks to the highly local character of the core excitations and the well defined separation in energy of unoccupied orbitals [25]. The interpretation of the NEXAFS spectra can then be operated in terms of the building block approach. This means that the features and the intensities of the spectra can be understood as a result of the additivity of the spectra referring to different subunits. The quantitative evaluation of the chemisorbed fraction of hydrogen is then obtained from a peak fitting procedure of the photoabsorption spectra after an accurate calibration and normalization of the experimental NEXAFS curves. This approach gives also information on the electronic configuration of the ns-C (e.g. the amount of sp^2 sites [26]).

2 Experimental

We have grown nanostructured carbon films by depositing cluster beams carried by a supersonic expansion. A detailed description of the deposition apparatus is presented in references [27,28]. Briefly it consists of three differentially evacuated chambers separated by skimmers. The apparatus operates in high vacuum regime (base pressure 1×10^{-7} Torr). During the deposition in the first chamber, which hosts the cluster source, the pressure is maintained in the range between 2×10^{-5} and 2×10^{-4} Torr. The second chamber is equipped with a manipulator on which a sample holder can intersect the beam along the axis of the apparatus. A Wiley-McLaren linear Time of Flight Mass Spectrometer is hosted in the third chamber collinear to the beam axis.

The cluster source is a Pulsed Microplasma Cluster Source (PMCS) [29] in which an aerodinamically confined plasma discharge ablates a graphite target. The plasma is obtained by the ionization of helium by means of pulsed discharge between two graphite electrodes. The sputtering of the target produces carbon atoms. The cluster-helium mixture is extracted through a nozzle to form a seeded supersonic beam. Working at typical conditions, we obtain a log-normal cluster mass distribution up to about 2000 atoms/cluster and peaked at about 600 atoms/cluster. A mass selection of the clusters exiting the source can be obtained by aerodynamical focusing. By forcing the particles entering the nozzle to follow a trajectory with sudden turns, only particles with a suitable Stoke's number will be able to go along the carrier gas streamlines [30]. This corresponds to the use of a bandpass filter. In particular for this work we have used a low bandpass filter depositing films where particles larger than roughly 2 nm have been eliminated. We have produced different films with decreasing mean cluster size distribution in order to characterize the influence of graphitic-like structure (large clusters) on the hydrogen uptake. The variation of cluster distribution also affects film density. Large clusters produce more porous films compared to small ones [28].

The NEXAFS experiments have been carried out at LURE Super-ACO storage ring on the SACEMOR experiment equipped with a high energy 10 m TGM monochromator (200 – 800 eV) of the beamline SA72. The energy resolution of the NEXAFS measurements was 0.2 eV at carbon *K*-edge. NEXAFS spectra have been acquired in Total Electron Yield (TEY) mode. No relevant differences have been observed with respect to corresponding spectra acquired in Partial Electron Yield (PEY) mode. This represents a strong indication that the film structure and hydrogen sorption are similar through the film depth. The NEXAFS signal has been obtained from the ratio between the sample signal collected by a channeltron and that of an 85% transmission gold coated grid giving the intensity of the incident beam. The spectra were acquired at the "magic angle" in order to obtain spectra independent of the synchrotron light polarization. A first series of spectra was obtained for as-deposited samples. Afterwards the samples were moved from the experimental chamber to the preparation chamber where they were subjected to thermal annealing at 400 °C for about 1 h in order to degas the adsorbed species (in particular water) with minor alterations of the film structure. After cooling down to room temperature the samples were reintroduced into the experimental chamber and a new series of spectra was acquired. Then the samples were moved again into the preparation chamber where they were exposed to molecular hydrogen (purity 99.9999%) at the pressure of 0.12 MPa for 3 h. Finally the samples were again brought into the experimental chamber and the last series of spectra was collected.

3 Data analysis

In the following paragraphs at first we present a detailed description of the initial steps performed in data analysis, i. e. calibration and normalization. Afterwards we describe the method for the effective evaluation of hydrogen uptake as obtained through a peak fitting procedure by assuming

a direct correlation between the area of the σ^*_{C-H} resonance and the amount of chemisorbed hydrogen, as the analysis of EELS spectra of hydrocarbons suggests.

3.1 Calibration

The raw spectra are obtained as the ratio between the sample signal collected by a channeltron and that of an 85% transmission gold-coated grid giving the intensity of the incident beam. According to the calibration method described in reference [26], the shifts in the energy scale of all the spectra of our collection, with respect to a particular one suitably chosen among them as a reference, can be determined by comparing the spectra of the gold-coated grid simultaneously acquired during each sample analysis. In these spectra, which in the range under consideration present mainly a signal linearly increasing with energy, minor structures are however present due to residual surface contaminations of the beam optics and of the gold grid. As a consequence, it is possible to uniquely determine for each spectrum the shift in the position of these structures on the energy scale, with respect to the reference one. This shift is automatically calculated by a numerical routine as the energy translation which, combined with a multiplication by a second-order polynomial in the energy (to account for variations in the intensity of the incident X-ray beam), provides the best overlap of the spectrum to the reference one.

The energy shifts were determined in this way in the various NEXAFS spectra as a function of the time of data acquisition. One can observe a somewhat regular behavior, on which a component of apparent daily periodicity is superimposed. Furthermore the displacements of the structures near the carbon threshold with those near the oxygen threshold vary as a function of time in almost exactly the same way, apart from the fact that the magnitude of the shifts in the O region is systematically larger by a factor about 3.3. This clearly indicates that the fluctuations in the behavior of the monochromator introduce a deformation of the energy scale. For simplicity, each spectrum has been however corrected by applying a constant shift over the whole energy range. This procedure appears to be sufficiently accurate when only the structures near the edge of a single element are to be considered in detail, as was the case for our spectra.

Independently of the reasons of the variations as a function of time, the regular behavior of the results obtained for our large set of spectra proves the reliability of our calibration method. As we have explained, it allows us to perform a relative calibration of the different spectra with respect to a chosen reference one. Of course, in order to obtain an absolute calibration, we fixed the energy scale of the HOPG spectrum by comparison with a reference taken from literature [31].

3.2 Normalization

In order to subtract the background from the spectra, we assume that the background can be identified with the straight line that best fits the behavior of the low-energy end of the spectrum, below the onset of the C transitions. However in most practical cases the determination of such a line is quite uncertain, due to the presence of additional minor structures in this region of the spectra. For this reason, we have initially considered only a particular spectrum of our collection characterized by a relatively wide low-energy plateau (Fig. 1). After background subtraction, the high-energy tail has been fitted by a decreasing exponential curve. Then the whole spectrum has been rescaled in such a way that the backward extrapolation of this exponential curve was normalized to 1 at the ionization potential (IP) placed at 289.4 eV [25] (see Fig. 1). After having normalized in this way this particular spectrum, we have taken it as a reference for the normalization of all the other spectra. Taking advantage of the fact that the great majority of the spectra have basically the same overall behavior, apart from the near edge features, we have prepared a numerical routine that, using as an input the background-subtracted and rescaled reference spectrum, calculates the background and the rescaling factor of all the other spectra so as to make them best overlap to the reference one, both in the low and high-energy regions. As an example, a typical result obtained by applying this procedure is shown in Figure 1. This procedure, since it makes simultaneously use of both the low and the high-energy regions of the spectrum, removes the ambiguities in the identification of the background, and thus provides a reliable criterion for a consistent normalization of all the spectra of the collection.

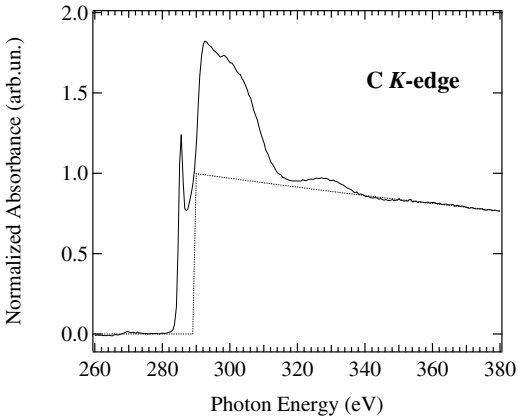

Fig. 1. C *K*-edge spectrum of a ns-C film after degassing and hydrogen exposure. Calibration, background subtraction and normalization procedures have been applied on the spectrum. The dotted curve is an *error function* (fixed width 1 eV) multiplied by a decreasing exponential curve normalized to 1 at the ionization potential.

3.3 Peak fitting and quantitative analysis

The spectra are fitted in the near-edge region as the superposition of an erf function ("error function") with a fixed width of 1 eV (to take into account the overall instrumental resolution), representing the step at the ionization

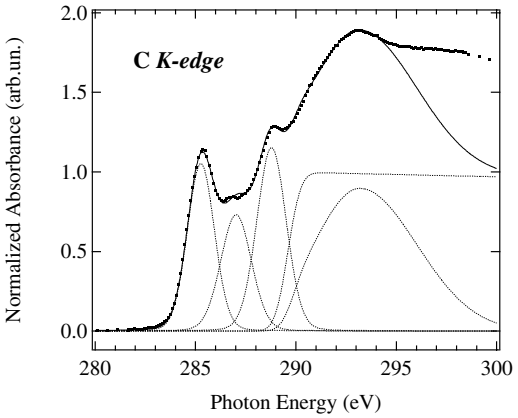

Fig. 2. Fitting of the near edge region of a carbon K-edge spectrum of as deposited ns-C film. Experimental data (solid circles) are fitted with three pseudo-Voigt functions in the pre-edge region, an asymmetric Gaussian function in the region just above the edge and a function representing the ionization step. The region above 294 eV has not been taken into account in the fitting procedure as shown by the behavior of the resulting fit curve (solid line) since no contribution to the pre-edge region can come from that part of the spectrum where multiple scattering processes are dominant.

threshold, a set of three pseudo-Voigt functions representing the peaks in the sub-threshold region, and an asymmetric Gaussian function describing the main peak above the threshold (Fig. 2). Due to the complex nature of ns-C films, the position of the IP can be slightly different among the various deposits. Thus in the fitting procedure we have left the position of the erf function free of varying between ±0.2 eV of the IP value. All the spectra can then be conveniently fitted by considering a reference ionization potential at 289.4 eV. In the sub-threshold region it is possible to recognize the peak related to the $\pi^*_{C=C}$ transition, located at 285.3 ± 0.2 eV (the number after the sign ± indicates the standard deviation of the distribution of the peak maxima for our entire set of spectra), a peak at about 287.1 eV and a peak associated with the σ^*_{C-H} transition at 288.8 ±0.07 eV. It is reasonable to assume that the area of this last peak is directly related to the amount of H chemically bonded to C in the sample. This assumption is supported by the analysis of EELS spectra of hydrocarbons reported in the literature. We have considered the curves for the oscillator strength reported by Hitchcock and Mancini [32] and, after performing an analogous fit, we have reported the areas of the peaks $\pi^*_{C=C}$ and σ^*_{C-H} (normalized with respect to the area of a fixed larger portion of the spectra) as a function respectively of the number of $\pi_{C=C}$ and σ_{C-H} bonds per C atom present in the molecule of each hydrocarbon, indicated with $n_{C=C}$ and n_{C-H} respectively. The analyzed hydrocarbons have been ethane, n-propane, n-butane, isobutane, cyclohexane, ethylene, propene, benzene, acethylene, propyne, 2-butyne [32]. In this way all the possible carbon hybridizations (sp^1, sp^2 and sp^3) have been taken into account. Further, in some of the considered molecules, diverse carbon atoms can be present with different hybridizations.

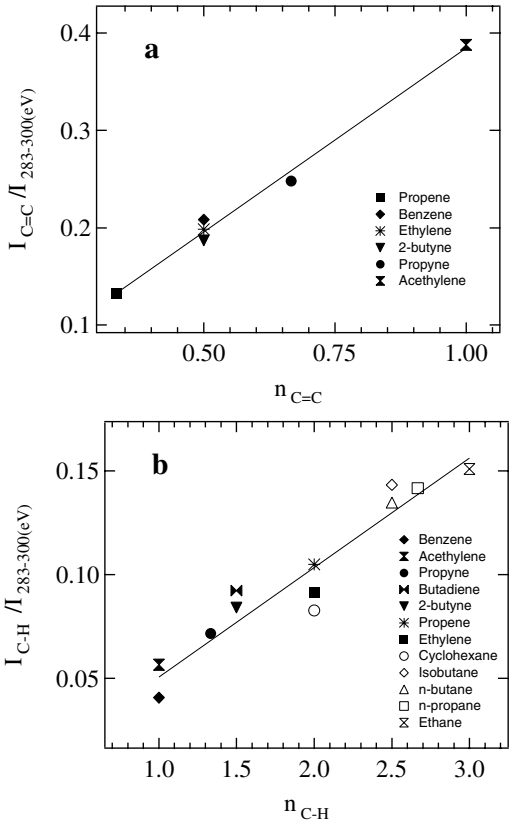

Fig. 3. Plots of peak area (normalized with respect to the area of the spectrum between 283 and 300 eV) as a function of the number of relative bonds per carbon atom of different molecules of hydrocarbons: a) normalized area of the π^* peak versus the number of $\pi_{C=C}$ bonds per carbon; b) normalized area of the σ^* peak versus the number of σ_{C-H} bonds per carbon atom.

For both types of bonds a linear relationship was found to hold with satisfactory approximation (Fig. 3a and Fig. 3b respectively).

For our NEXAFS data, the direct comparison of spectra acquired on the same samples before and after heat treatments and hydrogen exposures clearly exhibits a definite trend in the variation of the height of the σ^*_{C-H} and $\pi^*_{C=C}$ peaks (Fig. 4). One can notice the strong reduction of the peak at 288.8 eV after the heat treatment, and its partial restoration after exposure to hydrogen atmosphere.

In order to perform a quantitative analysis, we have considered that, in analogy with the results for hydrocarbons shown in Figs. 3a and 3b, the average amount $n_{C=C}$ of $\pi_{C=C}$ bonds per C atom in each sample is proportional to the ratio between the area $A_{C=C}$ of the $\pi^*_{C=C}$ peak and the area A_0 of a fixed larger portion of the spectra:

$$n_{C=C} = \alpha_{C=C} \frac{A_{C=C}}{A_0} \quad , \tag{1}$$

where $\alpha_{C=C}$ is a proportionality factor independent of the particular sample considered. A spectrum acquired on a specimen of Highly Oriented Pyrolytic Graphite (HOPG)

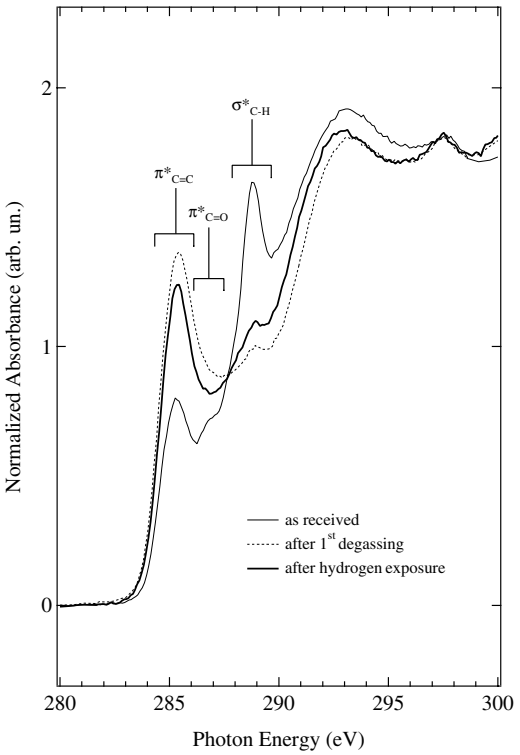

Fig. 4. Normalized NEXAFS C K-edge spectra for the sample A (see Tab. 1): as received (thin solid line); after thermal annealing (400° C for about 1 h in UHV) (dashed line) and after exposure to molecular hydrogen (pressure 0.12 MPa for 3 hours at room temperature in UHV) (thick solid line).

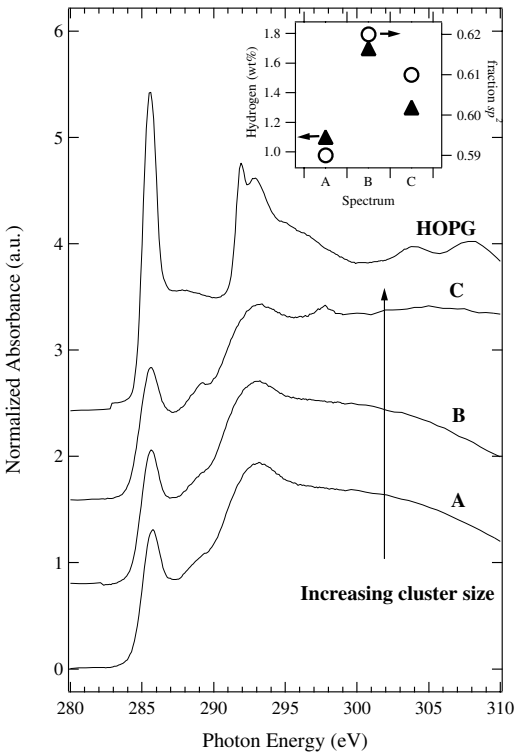

Fig. 5. Normalized carbon K-edge NEXAFS spectra after degassing and hydrogen exposure of samples grown with different precursor size distribution (see Tab. 1). As a reference, the spectrum of HOPG is also reported. In the inset the hydrogen uptake (evaluated by comparison with the spectra of the same samples prior to exposure) and sp^2 fraction are reported.

is representative for a 100% sp^2 sample ($n_{\mathrm{C=C}}^{\mathrm{HOPG}} = 0.5$, i.e. there is a $\pi_{\mathrm{C=C}}$ bond every two carbon atoms). Therefore it was possible to determine $\alpha_{\mathrm{C=C}}$ as

$$\alpha_{\mathrm{C=C}} = 0.5\,\frac{A_0^{\mathrm{HOPG}}}{A_{\mathrm{C=C}}^{\mathrm{HOPG}}} \ , \qquad (2)$$

and, by substituting equation (2) into equation (1), to estimate the sp^2 percentage in all the other samples, according to the relation:

$$f_{sp^2} \equiv 2n_{\mathrm{C=C}} = \frac{A_{\mathrm{C=C}}}{A_0}\,\frac{A_0^{\mathrm{HOPG}}}{A_{\mathrm{C=C}}^{\mathrm{HOPG}}} \ , \qquad (3)$$

which basically corresponds to the criterion already proposed by Fallon et al. [33]. Again in analogy with the results obtained for hydrocarbons, the number $n_{\mathrm{C-H}}$ of $\sigma_{\mathrm{C-H}}$ bonds is linearly related to the area $A_{\mathrm{C-H}}$ of the $\sigma^*_{\mathrm{C-H}}$ peak:

$$n_{\mathrm{C-H}} = \alpha_{\mathrm{C-H}}\frac{A_{\mathrm{C-H}}}{A_0} - \beta \ . \qquad (4)$$

The parameter $\alpha_{\mathrm{C-H}}$ in this relation has been determined by assuming its ratio to $\alpha_{\mathrm{C=C}}$ to be the same as for the corresponding parameters previously derived from the EELS spectra of Hitchcock and Mancini [32]. This gives:

$$\alpha_{\mathrm{C-H}} = \gamma\,\alpha_{\mathrm{C=C}} \ , \qquad (5)$$

where, since the inverse angular coefficients of the two straight lines which fit the data points of Figures. 3a and b are given respectively by $\alpha_{\mathrm{C=C}}^{\mathrm{EELS}} = 2.60\pm0.13$ and $\alpha_{\mathrm{C-H}}^{\mathrm{EELS}} = 19.2\pm1.8$, one obtains $\gamma = \alpha_{\mathrm{C-H}}^{\mathrm{EELS}}/\alpha_{\mathrm{C=C}}^{\mathrm{EELS}} = 7.4\pm0.8$. The term β on the right-hand side of equation (4) represents instead some additional contribution not necessarily related to the presence of H, which has been introduced to account for the fact that also for the spectra acquired after thermal degassing a nonvanishing area is attributed to this peak by the numerical fitting routine. Since the experimental environment was very clean (see details in Experimental section) we can guess that, whatever the origin of this contribution, for a given sample it does vary during the hydrogen exposure and subsequent analysis. Therefore this term cancels out when calculating the difference between $n_{\mathrm{C-H}}$ after and before the exposure, and even without the knowledge of β we are able with this procedure to estimate the number of $\sigma_{\mathrm{C-H}}$ bonds which are formed during the hydrogen exposure.

4 Results and discussion

The normalized carbon K-edge NEXAFS spectra of the investigated samples after thermal annealing and hydrogen exposure are reported in Figure 5, together with a reference spectrum of HOPG. As previously described, in

Table 1. Results of the fits of the spectra of Figure 5 and calculated values of hydrogen uptake and sp^2 fraction.

Spectrum	Area $\pi^*_{C=C}$	E $\pi^*_{C=C}$ (eV)	FWHM $\pi^*_{C=C}$	Area σ^*_{C-H}	E σ^*_{C-H} (eV)	FWHM σ^*_{C-H}	Area $_{(283-300)\ eV}$	f_{sp^2}	H(wt%)
A	1.95	285.27	1.58	2.13	288.87	1.73	23.41	0.59	1.1
B	2.03	285.25	1.57	2.24	288.84	1.63	23.53	0.62	1.7
C	2.02	285.29	1.55	2.04	288.87	1.73	23.70	0.61	1.3

the pre-edge part of the spectra three main features can be observed, i.e. the $\pi^*_{C=C}$ resonance at 285.3 eV, a peak at 287.1 eV, and the σ^*_{C-H} resonance at 288.8 eV. The first peak corresponds to the 1s $\rightarrow \pi^*$ transition and is mainly ascribable to carbon atoms in sp^2 bonding configuration. Nearby this resonance there should also be π^* antibonding states originating from *sp* hybridized C atoms. However it should be pointed out that the amorphous nature of the ns-C films gives rise to a broadening of the peak that may conceal other energetically close contributions. The attribution of the second peak is rather ambiguous. However this π^* state appears to be mainly related to bonds of C with oxygen containing contaminants [25]. In fact after annealing this peak is strongly reduced and this is accompanied by a decrease at O *K*-edge spectra ($\sim$ 530 eV) of the feature due to O bonded with C (not shown). The adventitious nature of oxygen containing species has been shown in core level photoemission spectroscopy where no evidence of oxygen inclusion during the deposition process has arisen [34]. Thus the exposure to atmosphere after film deposition can be recognized as the main source of the contamination since the vacuum in the analysis and treatment chambers was kept good along the measurement shift. The peak at 288.8 eV is identified as 1s$\rightarrow \sigma^*_{C-H}$ transitions for carbon bonded to hydrogen. The quantitative analysis of the spectra described above, i.e. evaluation of the sp^2 fraction and of the hydrogen content, can then be applied. As a consequence of the heating, the σ^*_{C-H} resonance is strongly reduced (see Fig. 4). The π^* peak instead appears more intense and wide indicating an increase in the sp^2 fraction up to about 0.8. This effect indicates the formation of C=C bonds even if the amorphous nature of the structure remains dominant. Subsequent exposure to pure molecular hydrogen partially restores the σ^*_{C-H} peak, suggesting the formation of a large number of C−H bonds. The amount of sp^2 sites is then reduced (the relative fraction decreases to about 0.7) accompanied by a narrowing of the π^* resonance. The sizable loss of sp^2 coordinated bonds in favor of C−H bonds represents a further indication that the principal mechanism of hydrogen uptake on carbon surfaces is chemisorption, as extensively discussed in references [35,36]. This restoration of the hydrogen can be favored by the defected nature of ns-C films, partially surviving also after moderate heating treatments. The exposure parameters could not be suitable for a relevant adsorption of hydrogen from the nanostructured carbon since, at present, information on the sorption kinetics is still missing. In any case, it is evident the capacity of these films to adsorb hydrogen and, under mild heating, to release it.

The spectra shown in Figure 5 correspond to samples grown with different geometrical configurations of the source, which are able to produce cluster size distributions with different median. In the figure the spectra are ordered as a function of increasing median size, ranging from about 400 atoms/cluster up to about 900 atoms/cluster. In Table 1 we report the results of the fits. From these data we have evaluated that the amount of chemisorbed hydrogen ranges between 1.1 and 1.7 wt.% for all the examined samples.

As regarding the associated error, we can rely upon a series of repeated spectra acquisitions for each sample before and after hydrogen exposure. The values of n_{C-H}, obtained from the analysis of these spectra, exhibit a standard deviation of about 0.02, which corresponds to an error for the hydrogen uptake of about 0.2 wt%.

In the inset of Figure 5 we have reported the obtained results for the samples shown in the graph either in terms of sp^2 fraction or of the effective hydrogen sorption. It is apparent how the different precursors size does not significantly influence the amount of chemisorbed hydrogen, even if the morphology of the films could be different. Thus this behavior is a further confirmation that the capability of dissociating hydrogen molecules is mainly related to the highly defective structure of the nanostructured carbon film. It should be also pointed out that, although the loading conditions have been not particularly severe (room temperature, exposure pressure 0.12 MPa for 3 h) the quantity of absorbed hydrogen is sizable.

5 Conclusions

We have developed a novel method for the quantitative evaluation of the chemisorbed fraction of hydrogen uptake in carbon nanostructures. It is based on the analysis of NEXAFS spectra at the carbon *K*-edge, by following the evolution of the $\pi^*_{C=C}$ and σ^*_{C-H} resonances. The method allows the characterization of even a low quantity of carbon material to expose to hydrogen ($< 1\,\mu$m). It is then possible to overcome the limit usually encountered with other techniques for measuring hydrogen storage capacity in carbon based materials. Moreover this experimental approach allows us to avoid some artifacts, mainly due to water contamination. In fact the effectiveness of the degassing process and likewise the absorption of oxygen containing species during hydrogen exposure can be directly monitored by acquiring X-ray absorption spectra at oxygen K-edge. Thus the reliability of the method lies not only in the data handling but also in the experimental procedure needed for the sample treatment and data acquisition. We are aware that with this method the physisorbed fraction is not assessed, however we have both theoretical calculations [24] and experimental evidence [23] showing

that this contribution can be considered negligible in our films. In further support of this, recent theoretical publications highlight that the physisorbtion can be neglected in nanotubes at room temperature [37] or in highly defected graphite [38]. We have applied this method to a series of ns-C films grown via supersonic cluster beam deposition with different experimental conditions. We have observed that hydrogen exposure of ns-C under mild conditions of temperature and pressure results in an uptake of about 1.5 wt.%. This value is comparable to the most recent data reported for different carbon nanostructures. On the basis of these results, we plan further investigations. In particular we will deposit films of ns-C with inclusion of metals, such as Pt, in order to improve the dissociation of hydrogen molecules and to favor the effective hydrogen uptake.

We acknowledge financial support from MIUR under project FIRB "Micro-strutture e nano-strutture a base di carbonio". The authors wish also to thank C. Laffon and Ph. Parent for their scientific and technical support at LURE facility.

References

1. A.C. Dillon, K.M. Jones, T.A. Bekkedahl, C.H. Kiang, D.S. Bethune, M.J. Heben, Nature **386**, 377 (1997)
2. A. Chambers, C. Park, R.T.K. Baker, N.M. Rodriguez, J. Phys. Chem. B **102**, 4253 (1998)
3. C. Park, P.E. Anderson, A. Chambers, C.D. Tan, R. Hidalgo, N.M. Rodriguez, J. Phys. Chem. B **103**, 10572 (1999)
4. Y.Y. Fan, B. Liao, M. Liu, Y.-L. Wei, M.-Q. Lu, H.-M. Cheng, Carbon **37**, 1649 (1999)
5. M. Hirscher, M. Becher, M. Haluska, F. von Zeppelin, X. Chen, U. Dettlaff-Weglikowska, S. Roth, J. Alloys Compd. **356-357**, 433 (2003)
6. S. Orimo, A. Züttel, L. Schlapbach, G. Majer, T. Fukunaga, H. Fujii, J. Alloys Compd. **356-357**, 716 (2003)
7. C. Nützenadel, A. Züttel, D. Chartouni, L. Schlapbach, Electroch. Solid-State Lett. **2**, 30 (1999)
8. S.-P. Chan, G. Chen, X. Gong, Z.-F. Liu, Phys. Rev. Lett. **87**, 205502/1 (2001)
9. K. Tada, S. Furuya, K. Watanabe, Phys. Rev. B **63**, 155405 (2001)
10. Y. Ma, Y. Xia, M. Zhao, M. Ying, Phys. Rev. B **65**, 155430/1 (2002)
11. G.G. Tibbetts, G.P. Meisner, C.H. Olk, Carbon **39**, 2291 (2001)
12. C. Liu, Q. Yang, Y. Tong, H. Cong, H. Cheng, Appl. Phys. Lett. **80**, 2389 (2002)
13. M. Ritschel, M. Uhlemann, O. Gutfleisch, A. Leonhardt, A. Graff, C. Taschner, J. Fink, Appl. Phys. Lett. **80**, 2985 (2002)
14. A. Züttel, C. Nützenadel, P. Sudan, P. Mauron, C. Emmenegger, S. Rentsch, L. Schlapbach, A. Weidenkaff, T. Kiyobayashi, J. Alloys Compd. **330-332**, 676 (2002)
15. R. Ströbel, Jörissen, T. Schliermann, V. Trapp, W. Schütz, K. Bohmhammel, G. Wolf, J. Garche, J. Pow. Sources **84**, 221 (1999)
16. M. de la Casa-Lillo, F. Lamari-Darkrim, D. Cazorla-Amoros, A. Linares-Solano, J. Phys. Chem. B **106**, 10930 (2002)
17. H. Zhu, X. Li, L. Ci, C. Xu, D. Wu, Z. Mao, Mat. Chem. Phys. **78**, 670 (2003)
18. M. Hirscher, M. Becher, J. Nanosci. Nanotech. **3**, 3 (2003)
19. Y. Ye, C.C. Ahn, C. Witham, B. Fultz, J. Liu, A.G. Rinzler, D. Colbert, K.A. Smith, R.E. Smalley, Appl. Phys. Lett. **74**, 2307 (1999)
20. M. Hirscher, M. Becher, M. Haluska, U. Dettlaff-Weglikowska, A. Quintel, G.S. Duesberg, Y.-M. Choi, P. Downes, M. Hulman, S. Roth, I. Stepanek, P. Bernier, Appl. Phys. A **72**, 129 (2001)
21. P. Milani, P. Piseri, E. Barborini, A. Podestà, C. Lenardi, J. Vac. Sci. Technol. A **19**, 2025 (2001)
22. D. Donadio, L. Colombo, P. Milani, G. Benedek, Phys. Rev. Lett. **83**, 776 (1999)
23. C. Lenardi, E. Barborini, V. Briois, L. Lucarelli, P. Piseri, P. Milani, Diamond Relat. Mater. **10**, 1195 (2001)
24. P. Piseri, E. Barborini, M. Marino, P. Milani, C. Lenardi, L. Zoppi, L. Colombo, J. Phys. Chem. B **108**, 5157 (2004)
25. J. Stöhr, *NEXAFS Spectroscopy* (Springer-Verlag, Berlin, 1992)
26. C. Lenardi, P. Piseri, V. Briois, C.E. Bottani, A. Li Bassi, P. Milani, J. Appl. Phys. **85**, 7159 (1999)
27. E. Barborini, P. Piseri, A. Li Bassi, A.C. Ferrari, C.E. Bottani, P. Milani, Chem. Phys. Lett. **300**, 633 (1999)
28. P. Milani, A. Podestà, P. Piseri, E. Barborini, C. Lenardi, C. Castelnovo, Diam. Relat. Mater. **10**, 240 (2001)
29. E. Barborini, P. Piseri, P. Milani, J. Phys. D: Appl. Phys. **32**, L105 (1999)
30. P. Piseri, A. Podestà, E. Barborini, P. Milani, Rev. Scient. Instrum. **72**, 2261 (2001)
31. P.E. Batson, Phys. Rev. B **48**, 2608 (1993)
32. A.P. Hitchcock, D.C. Mancini, J. Electron Spectrosc. **67**, 1 (1994)
33. P.J. Fallon, V.S. Veersamy, C A. Davis, J. Robertson, G.A.J. Amaratunga, W.J. Milne, J. Koskinen, Phys. Rev. B **48**, 4777 (1993)
34. E. Magnano, C. Cepek, M. Sancrotti, F. Siviero, S. Vinati, C. Lenardi, E. Barborini, P. Piseri, P. Milani, Phys. Rev. B **67**, 125414 (2003)
35. R.C. Bansal, F.J. Vastola, P.L. Walker Jr., Carbon **9**, 185 (1971), and references therein
36. J.B. Donnet, R. Bansal, M.J. Wang, *Carbon black: Science and Technology* (Dekker, New York, 1993)
37. J. Li, T. Furuta, H. Goto, T. Ohashi, Y. Fujiwara, S. Yip, J. Chem. Phys. **119**, 2376 (2003)
38. S. Letardi, M. Celino, F. Cleri, V. Rosato, M. Volpe, Surf. Sci. **496**, 33 (2002)